Geophysical Research Letters

RESEARCH LETTER
10.1029/2024GL110787

Role of Ion Dynamics in Electron-Only Magnetic Reconnection

Yundan Guan[1], Quanming Lu[1,2,3], San Lu[1,2,3], Yukang Shu[1], and Rongsheng Wang[1,2,3]

[1]CAS Center for Excellence in Comparative Planetology, CAS Key Lab of Geospace Environment, School of Earth and Space Sciences, University of Science and Technology of China, Hefei, China, [2]Deep Space Exploration Laboratory, Hefei, China, [3]Collaborative Innovation Center of Astronautical Science and Technology, Harbin, China

Key Points:

- Electrons are not accelerated to electron Alfvén speed in electron-only magnetic reconnection
- Deceleration of electron outflow caused by in-plane Hall electric field should not be ignored

Supporting Information:

Supporting Information may be found in the online version of this article.

Correspondence to:

Q. Lu and S. Lu,
qmlu@ustc.edu.cn;
lusan@ustc.edu.cn

Citation:

Guan, Y., Lu, Q., Lu, S., Shu, Y., & Wang, R. (2024). Role of ion dynamics in electron-only magnetic reconnection. *Geophysical Research Letters*, *51*, e2024GL110787. https://doi.org/10.1029/2024GL110787

Received 12 JUN 2024
Accepted 23 SEP 2024

© 2024. The Author(s).
This is an open access article under the terms of the Creative Commons Attribution License, which permits use, distribution and reproduction in any medium, provided the original work is properly cited.

Abstract Standard magnetic reconnection couples with both ions and electrons on different scales. Recently, a new type of magnetic reconnection, electron-only reconnection without the coupling of ions, has been observed in various plasma environments. Standard reconnection typically has a reconnection outflow velocity of about one Alfvén speed. According to the scaling analysis, the electron outflow velocity is expected to be about one electron Alfvén speed in electron-only reconnection. However, observations and simulations both find that the electron outflows are much slower than the electron Alfvén speed. In this letter, by performing two-dimensional particle-in-cell simulations, we show that this is because ions play a role in electron-only reconnection. The ions move slower than the electrons in the outflow direction, and such charge separation forms an in-plane Hall electric field, which prevents the electrons from being accelerated to the electron Alfvén speed in electron-only reconnection.

Plain Language Summary Magnetic reconnection is a fundamental plasma process during which magnetic field line topologies change and magnetic energy transfers to plasma kinetic and thermal energy. In standard collisionless magnetic reconnection, ions and electrons are both heated and accelerated to form high-speed outflow. Theoretical analyses have been performed to successfully explain the fast outflow speed in standard magnetic reconnection. Recently, a new type of magnetic reconnection, electron-only reconnection (in which there is no obvious ion heating and acceleration) has been reported to occur in various plasma environments. However, the same scaling analyses performed in electron-only reconnection overestimate the outflow speed in the electron-only reconnection by a factor of ∼10. Here, by performing two-dimensional (2-D) particle-in-cell (PIC) simulations, we show that the overestimation is due to the neglect of the role of ions. Because of the in-plane Hall electric field caused by charge separation, electron outflow in electron-only reconnection cannot be accelerated to the expected value.

1. Introduction

Magnetic reconnection, a topological change in magnetic field lines, provides a physical mechanism for conversion from magnetic energy to plasma kinetic energy (Birn & Priest, 2007; Hesse & Cassak, 2020; S. Wang & Lu, 2019; Yamada et al., 2010). Magnetic reconnection has been widely believed to be responsible for various explosive phenomena throughout the universe, such as solar flares, coronal mass ejections, and Earth's magnetospheric storms and substorms (Angelopoulos et al., 2008; Burch et al., 2016; Lin & Forbes, 2000; Q. Lu et al., 2022; Masuda et al., 1994; Torbert et al., 2018). Magnetic reconnection in most plasma environments is collisionless, where the diffusion of the magnetic field is caused by the kinetic effects of ions and electrons. In standard magnetic reconnection, the diffusion of the magnetic field occurs both in a larger-scale ion diffusion region and a smaller-scale electron diffusion region, and the electron diffusion region (EDR) is embedded at the center of the ion diffusion region (IDR) (Birn et al., 2001; Birn & Hesse, 2001; Borg et al., 2005; Burch et al., 2016; Q. Lu et al., 2010; Nagai et al., 2001; Pritchett, 2001; Shay et al., 2001).

Recently, a new type of magnetic reconnection, electron-only magnetic reconnection, has been observed in space and laboratory plasmas (Gingell et al., 2020; Hubbert et al., 2021, 2022; Man et al., 2020; Phan et al., 2018; Sang et al., 2022; Shi et al., 2022a, 2022b; Stawarz et al., 2019, 2022; Wang et al., 2018, 2020). Different from standard reconnection, electron-only reconnection exhibits only the electron dynamics, whereas the ions do not seem to be coupled, that is, there is no obvious ion heating and acceleration in electron-only reconnection (Guan et al., 2023; Lu S. et al., 2020b, 2022; Pyakurel et al., 2019).

In standard reconnection, by considering the momentum equation with Lorentz force and performing scaling analysis to the diffusion region, the velocity of the ion outflow is about one Alfvén speed V_A (where $V_A = B_0/\sqrt{\mu_0 m_i n_0}$, B_0 is the magnitude of the ambient magnetic field, and n_0 is the peak density of the current sheet), and the reconnection rate is about $0.1B_0V_A$ (Cassak et al., 2017; Hesse et al., 2009; Y. Liu et al., 2017). Therefore, by applying a similar analysis to the electrons and the EDR, it is natural to expect that in the electron-only reconnection, the speed of the electron outflow is about one electron Alfvén speed V_{Ae} (where $V_{Ae} = B_0/\sqrt{\mu_0 m_e n_0} = \sqrt{m_i/m_e}V_A$, m_i/m_e is the ion-to-electron mass ratio), and the reconnection rate is about $0.1B_0V_{Ae}$ (i.e., $0.1\sqrt{m_i/m_e}B_0V_A$). However, the electron outflow speed and reconnection rate obtained from PIC simulations and observations of electron-only reconnection can be much lower than the expected values above (Bessho et al., 2022; Burch et al., 2020; Guan et al., 2023; Ng et al., 2022; Pyakurel et al., 2019; Stawarz et al., 2022). To explain this controversy, in this letter, by performing 2-D PIC simulations of electron-only reconnection, we find that the ion dynamics plays an important role by forming an in-plane Hall electric field, which leads to a much slower electron outflow and a much smaller reconnection rate than expected.

2. Simulation Model

In this paper, we use a 2D PIC simulation code, which has been successfully applied to study magnetic reconnection (C. Chang et al., 2021; X. Fu et al., 2006; C. Huang et al., 2010, 2015; Q. Lu et al., 2010). The simulation is 2.5-dimensional, that is, the simulation domain is 2-dimensional and the particle velocity is 3-dimensional. The simulation is in the x-z plane. The initial configuration is a charged, electron-dominant current sheet (S. Lu et al., 2020a). The magnetic fields are normalized to the magnitude of the upstream magnetic field B_0, density to the maximum of the current sheet density n_0, time to Ω_i^{-1} (where $\Omega_i = eB_0/m_i$ is the ion gyrofrequency), lengths to the ion inertial length $d_i = m_i/(\mu_0 n_0 e^2)$, velocities to the Alfvén speed $V_A = B_0/\sqrt{\mu_0 m_i n_0}$ (also referred to as the ion Alfvén speed), electric fields to $E_0 = B_0V_A$, and temperatures to $m_iV_A^2$.

In the simulation, an electron-dominant current sheet with a high ion temperature is considered. The ratio between the initial ion and electron drift velocities is $V_i/(-V_e) = 1/9$, and the initial half-width of the current sheets δ is $0.06d_i \approx 2.6d_e$. The initial ion temperature $T_i = 0.45m_iV_A^2$ and the initial electron temperature $T_e = 0.05m_iV_A^2$. The initial magnetic field is an antiparallel configuration. The upstream background density $n_b = 0.1n_0$. The method of calculating the initial magnetic field, the initial electric field, and the initial plasma density is demonstrated in the previous work (S. Lu et al., 2020a). The grid size is $dx = dz = 0.005d_i$, and the grid number is $N_x = N_z = 300$. Therefore the size of the simulation domain $L_x = L_z = L = 1.5d_i$. The time step is $dt = 10^{-5}\Omega_i^{-1}$.

The ion-to-electron mass ratio is $m_i/m_e = 1{,}836$, and the speed of light is $c = 50V_A$. We use 1,000 particles per species per cell to represent n_0 in the simulation. No initial perturbation is added to the initial magnetic flux. Periodic boundary conditions are used in the x direction. Perfect conducting boundary conditions for electromagnetic fields and reflecting boundary conditions for particles are used in the z direction.

3. Simulation Results

Figure 1 shows the overview of magnetic reconnection in this simulation. Figures 1a and 1b show the outflows in the reconnection at $t = 0.24\Omega_i^{-1}$. There is an extremely slow ion outflow, $V_{ix} < 0.03V_A$, while the electron outflow is fast and super-Alfvénic, $V_{ex} = 2V_A \approx 0.05V_{Ae}$. Compared to the initial temperature, the ions are not heated, but the electron temperature increases by about $0.01m_iV_A^2$, as shown in Figures 1c and 1d. Therefore, the ions are not heated or accelerated significantly, but the electrons are heated and accelerated to super-Alfvénic speeds. This demonstrates that magnetic reconnection here is electron-only. Note that although the electron outflow velocity $V_{ex} = 2V_A \approx 0.05V_{Ae}$ is super-Alfvénic, it is more than 10 times slower than the electron Alfvén speed. The time history of the reconnection rate in the electron-only reconnection is shown in Figure 1e. The reconnection rate is defined as the reconnection electric field E_y at the reconnection site. The whole reconnection lasts for about 0.5 Ω_i^{-1}, and the maximum reconnection rate reaches $0.27B_0V_A$ at $t = 0.24\Omega_i^{-1}$. On the other hand, the maximum reconnection rate in the standard reconnection of the Charged Current Sheet is $0.06B_0V_A$ (S. Lu et al., 2020a). Although the reconnection rate of about $0.27B_0V_A$ in the electron-only reconnection is much faster than that in the standard reconnection, it is equivalent to $0.006B_0V_{Ae}$, more than 10 times slower than $0.1B_0V_{Ae}$.

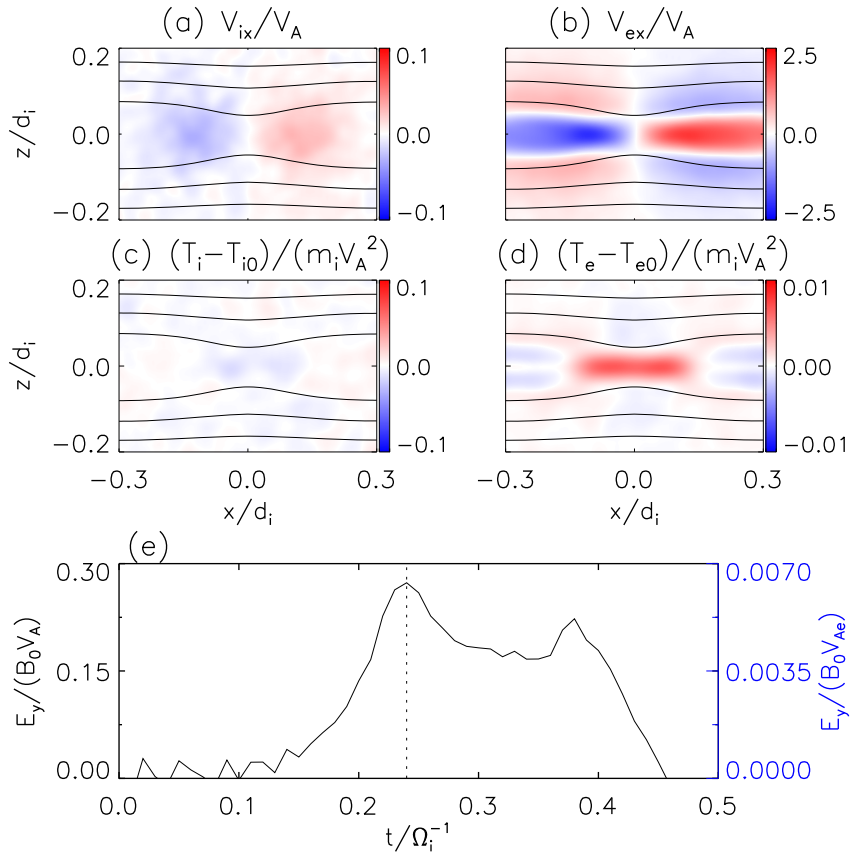

Figure 1. (a–d) Overview of the reconnection at $t = 0.24\Omega_i^{-1}$. (a) The ion bulk velocity in the x direction V_{ix}. (b) The electron bulk velocity in the x direction V_{ex}. (c) The increment of ion temperature. (d) The increment of electron temperature. (e) Time evolution of the reconnection rate calculated by the reconnection electric field E_y (the black solid line). $t = 0.24\Omega_i^{-1}$ is presented by the black dashed line in panel (e).

To explain why the electron outflow velocity is much slower than the electron Alfvén speed, we consider the x component of the electron momentum equation

$$m_e\frac{\mathrm{d}V_{ex}}{\mathrm{d}t} = -eE_x - e(\mathbf{V}_e\times\mathbf{B})_x - \left(\nabla\cdot\vec{\boldsymbol{P}}_e\right)_x/n_e. \quad (1)$$

The terms on the right side of Equation 1 are the electric field force term, the Lorentz force term, and the electron pressure gradient force term, respectively. As shown in Figures 2a–2d, the Lorentz force accelerates the electrons, while the electric field force and the electron pressure gradient force decelerate the electron outflow. For the two terms that decelerate the electrons, the electron pressure gradient force term is small and negligible, and the electric field force term compensates most of the Lorentz force term. This is also shown in the integral of the force terms along $z = 0$ (Figure 2e). Figure 2f plots the integrals of the left side and the right side of the electron momentum equation, and we can find that the two sides of the equation are almost balanced, verifying the accuracy of the calculation for the force terms. Therefore, it is the electric field E_x that prevents the electrons from being accelerated to the electron Alfvén speed V_{Ae}.

Figure 3a shows the reconnection electric field at $t = 0.24\Omega_i^{-1}$. The reconnection electric field E_y is confined to a small region, which is on the sub-ion scale. The reconnection electric field on this small scale is not sufficient to accelerate or heat ions but is sufficient for electron acceleration and heating. As shown in Figure 3b, the EDR has a multi-scale structure: an inner EDR where the non-ideal electric field is positive $(\mathbf{E}+\mathbf{V}_e\times\mathbf{B})_y > 0$ and an outer EDR where the non-ideal electric field is negative $(\mathbf{E}+\mathbf{V}_e\times\mathbf{B})_y < 0$ (Karimabadi et al., 2007; Shay et al., 2007).

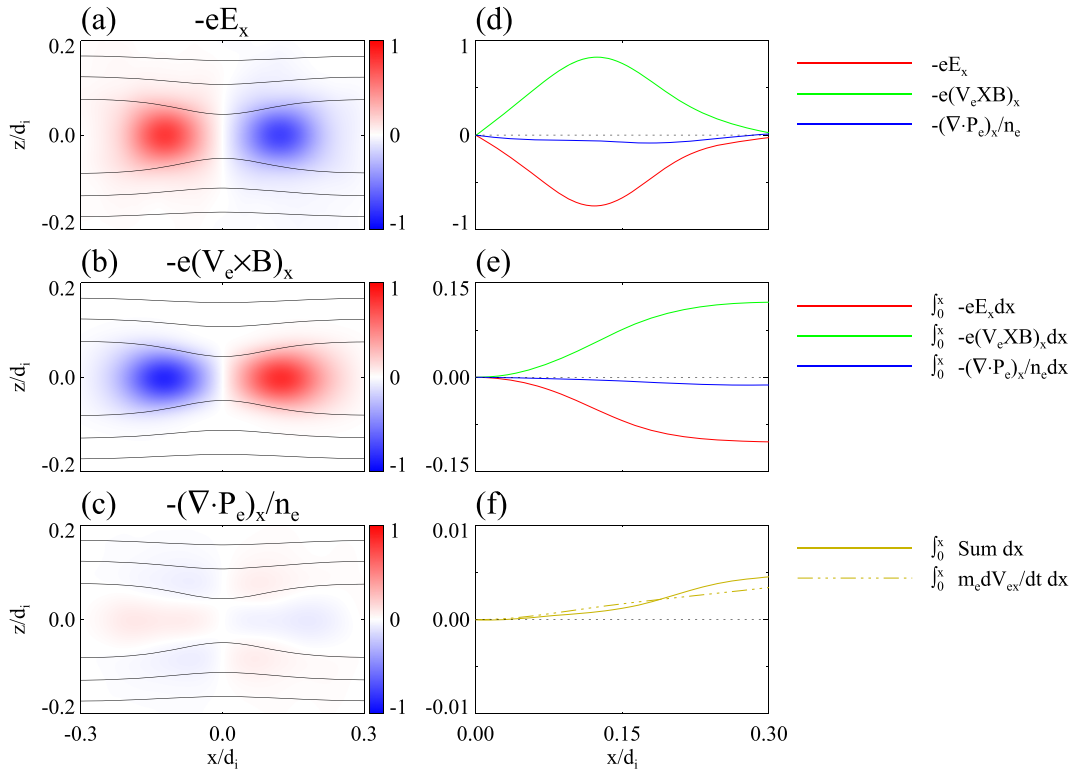

Figure 2. (a–c) The x-component of the force terms on the right side of the electron momentum equation at $t = 0.24\Omega_i^{-1}$. (a) The electric field force term. (b) The Lorentz force term. (c) The electron pressure gradient force term. (d) The profiles of forces on electrons along $z = 0$. (e) The integral of the force terms along $z = 0$. (f) The integral of the right side (sum of force terms) and the left side (inertia term) of the electron momentum equation along $z = 0$.

The inner EDR has formed with a half-length of $0.12d_i$, and the reconnection electric field at the boundary of the inner EDR is close to that at the reconnection site (Figures 3a and 3b). Thus we can use E_y at the boundary between the inner and outer EDR to represent the reconnection rate. At the boundary, $(\mathbf{E} + \mathbf{V}_e \times \mathbf{B})_y = 0$ is satisfied, so at this location, the reconnection rate can be described as $E_y = -(\mathbf{V}_e \times \mathbf{B})_y = V_{ex}B_z$, as shown in

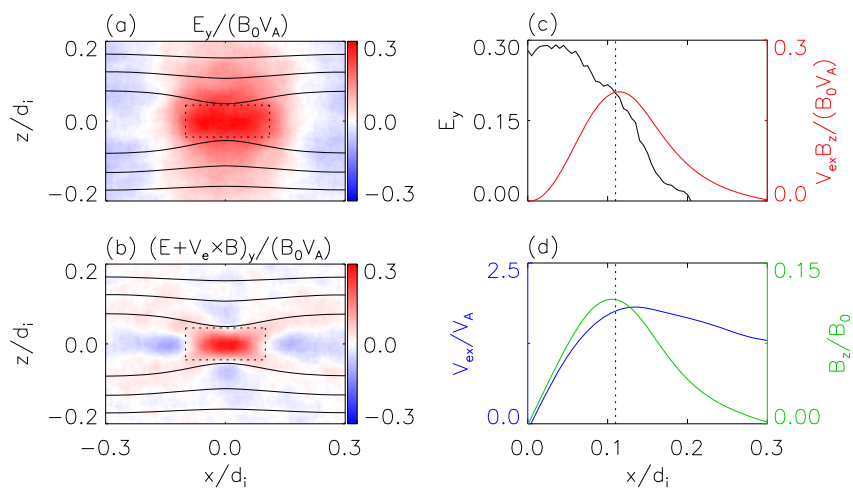

Figure 3. (a) The reconnection electric field E_y at $t = 0.24\Omega_i^{-1}$. (b) The non-ideal electric field $(\boldsymbol{E} + \boldsymbol{V_e} \times \boldsymbol{B})_y$ at $t = 0.24\Omega_i^{-1}$. (c) The profiles of the reconnection electric field E_y (black solid line) and the $V_{ex}B_z$ term (red line) along $z = 0$. (d) The profiles of the B_z pileup (green line) and the electron outflow velocity V_{ex} (blue line) along $z = 0$. The black dashed lines present the inner EDR boundary.

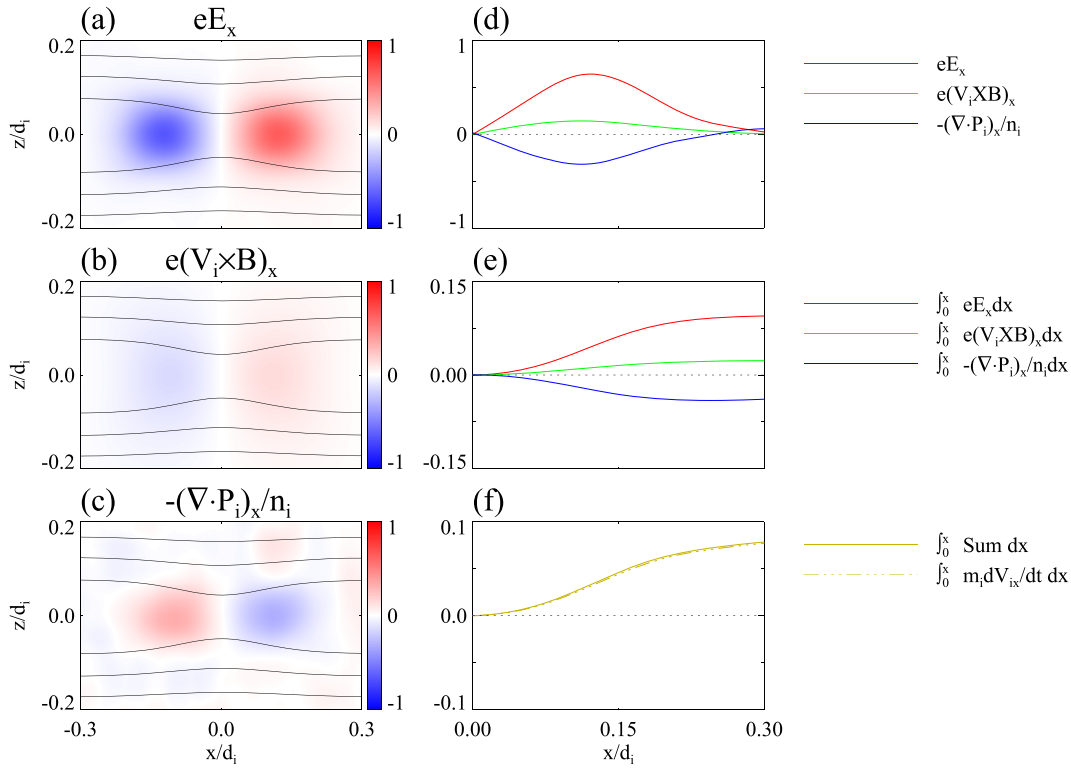

Figure 4. (a–c) The x-component of the force terms on the right side of the ion momentum equation at $t = 0.24\Omega_i^{-1}$. (a) The electric field force term. (b) The Lorentz force term. (c) The ion pressure gradient force term. (d) The profiles of forces on ions along $z = 0$. (e) The integral of the force terms along $z = 0$. (f) The integral of the right side (sum of force terms) and the left side (inertia term) of the ion momentum equation along $z = 0$.

Figure 3c. Although B_z piles up and reaches $0.1B_0$, because the electron outflow $V_{ex} = 2V_A \approx 0.05V_{Ae}$ is much slower than V_{Ae}, the reconnection rate $E_y = V_{ex}B_z \approx 0.05V_{Ae} \cdot 0.1B_0$ is also much slower than $0.1B_0V_{Ae}$ (Figure 3d).

A similar force analysis is performed for ions to investigate the ion flow. The x component of the ion momentum equation is written as

$$m_i \frac{\mathrm{d}V_{ix}}{\mathrm{d}t} = eE_x + e(\mathbf{V}_i \times \mathbf{B})_x - \left(\nabla \cdot \vec{\boldsymbol{P}}_i\right)_x / n_i. \tag{2}$$

As shown in Figures 4a–4e, both the electric field force and Lorentz force can accelerate the ions, while the ion pressure gradient force tends to decelerate the ion outflow. In the electron-only reconnection, the localized E_y on the sub-ion scale cannot sufficiently accelerate the ions, and the IDR on the ion inertial length scale is not formed, thus the Lorentz force term $(\mathbf{J}_i \times \mathbf{B})_x / n_i \approx V_{iy}B_z$ is weak. The acceleration of ions is mainly caused by the electric field E_x. (Also, the integrals of the left side and the right side of the ion momentum equation are almost balanced, as shown in Figure 4f.) Nevertheless, in the absence of strong support from the Lorentz force, the ion outflow remains slow in electron-only reconnection, much slower than the ion Alfvén speed.

4. Conclusions and Discussion

In this letter, by performing a 2-D PIC simulation, we show that because ions are barely affected by electron-only magnetic reconnection, they move much slower than the electrons in the outflow direction, which causes charge separation and thus forms a Hall electric field (see Figure S1 in Supporting Information S1). This Hall electric field corresponds to a backward electric force, which prevents the electrons from being accelerated to one electron Alfvén speed V_{Ae}. For the same reason, the reconnection rate in electron-only reconnection cannot reach

$0.1B_0V_{Ae}$. On the other hand, the ions are forced to flow away slowly from the reconnection site due to the Hall electric field.

Previous simulations by Pyakurel et al. (2019) show that electron-only reconnection occurs when the simulation domain size is no more than $10d_i$. Further simulations by Guan et al. (2023) find that the ion gyroradius is a more appropriate reference scale, and electron-only reconnection occurs when the simulation domain size is comparable to the ion gyroradius. In that work, using force-free configuration, the ion motion is the gyration under guide fields, and the ion trajectories are used to explain why electron-only reconnection occurs when the size of the simulation domain is comparable to the ion gyroradius. In this study, under antiparallel configuration, the ion motion near the center of the current sheet is a bounce motion, whose width is given by $\lambda_{iz} = \left[\frac{2m_iT_i}{e^2\left(\frac{\partial B_x}{\partial z}\right)^2}\right]^{\frac{1}{4}}$ (Hesse et al., 2011), and in this case $\lambda_{iz} = 0.26d_i$. The scale of the ion motion is comparable to the size of the reconnection electric field, so the ions cannot be sufficiently accelerated and heated, and the Lorentz force on ions is weak, leading to electron-only reconnection. Both explanations express that when the scale size of the reconnection electric field is comparable to the spatial scale of the ion motion, electron-only reconnection occurs. The explanations are essentially consistent. Moreover, the smaller the domain is, the faster the reconnection rate is, and it is again noted that the domain size L here should be decided by the scale size of the ion motion R_i instead of the ion inertial length d_i (Guan et al., 2023). In the force-free configuration used in Pyakurel et al. (2019) with a large guide field $B_g = 8B_0$ and a high ion temperature $T_i = 115.16m_iV_A^2$, R_i is the ion gyroradius, that is, $R_i = \rho_i = \sqrt{2m_iT_i}/(eB) = 1.88d_i$, and the domain size of the electron-only case is $L = 2.56d_i$, that is $L \approx 1.4R_i$. On the other hand, in this letter with antiparallel configuration, we have $R_i = \lambda_{iz} = 0.26d_i$, and the domain size of $L = 1.5d_i$ is thus $L \approx 5.8R_i$, which is larger than that in Pyakurel et al. (2019), and therefore the reconnection rate is lower.

Based on the above simulation results, we can demonstrate the process of energy conversion in electron-only reconnection. The released magnetic energy is first converted to electron thermal and bulk kinetic energies to heat and accelerate the electrons whereas the ions are barely heated or accelerated (Figure 1). Such process forms charge separation and thus the Hall electric field (Figure S1 in Supporting Information S1), during which the electron kinetic energy is converted to electric field energy. At the same time, the Hall electric field decelerates the electrons and accelerates the ions, so the electric field energy is then converted to the ion kinetic energy. The electric field acts as an intermedia in this process, and its energy can be comparable to the ion kinetic energy, and eventually, almost all of it is converted into the ion kinetic energy (Figure S2 in Supporting Information S1). However, the complete energy budgets during electron-only reconnection, especially the heating process, need closer examinations of the energy fluxes, such as the enthalpy flux and the heat flux, which will be left for future investigations.

Data Availability Statement

The simulation data (Guan, 2024) used to plot the figures in this paper can be downloaded from "National Space Science Data Center, National Science & Technology Infrastructure of China".

Acknowledgments
This work was supported by the NSFC Grants 42230201 and 42274196, National Key Research and Development Program of China (2022YFA1604600), the, and the Strategic Priority Research Program of the Chinese Academy of Sciences, Grants XDB 41000000 and 0560000.

References

Angelopoulos, V., McFadden, J. P., Larson, D., Carlson, C. W., Mende, S. B., Frey, H., et al. (2008). Tail reconnection triggering substorm onset. *Science*, *321*(5891), 931–935. https://doi.org/10.1126/science.1160495

Bessho, N., Chen, L., Stawarz, J. E., Wang, S., Hesse, M., Wilson, L. B., et al. (2022). Strong reconnection electric fields in shock-driven turbulence. *Physics of Plasmas*, *29*(4), 042304. https://doi.org/10.1063/5.0077529

Birn, J., Drake, J. F., Shay, M. A., Rogers, B. N., Denton, R. E., Hesse, M., et al. (2001). Geospace Environmental Modeling (GEM) magnetic reconnection challenge. *Journal of Geophysical Research*, *106*(A3), 3715–3719. https://doi.org/10.1029/1999JA900449

Birn, J., & Hesse, M. (2001). Geospace Environment Modeling (GEM) magnetic reconnection challenge: Resistive tearing, anisotropic pressure and Hall effects. *Journal of Geophysical Research*, *106*(A3), 3737–3750. https://doi.org/10.1029/1999JA001001

Birn, J., & Priest, E. R. (2007). *Reconnection of magnetic fields: Magnetohydrodynamics and collisionless theory and observations*. Cambridge University Press.

Borg, A. L., Oieroset, M., Phan, T. D., Mozer, F. S., Pedersen, A., Mouikis, C., et al. (2005). Cluster encounter of a magnetic reconnection diffusion region in the near-Earth magnetotail on September 19, 2003. *Geophysical Research Letters*, *32*(19), L19105. https://doi.org/10.1029/2005gl023794

Burch, J. L., Torbert, R. B., Phan, T. D., Chen, L. J., Moore, T. E., Ergun, R. E., et al. (2016). Electron-scale measurements of magnetic reconnection in space. *Science*, *352*(6290), aaf2939. https://doi.org/10.1126/science.aaf2939

Burch, J. L., Webster, J. M., Hesse, M., Genestreti, K. J., Denton, R. E., Phan, T. D., et al. (2020). Electron inflow velocities and reconnection rates at Earth's magnetopause and magnetosheath. *Geophysical Research Letters*, *47*(17), e2020GL089082. https://doi.org/10.1029/2020GL089082

Cassak, P. A., Liu, Y. H., & Shay, M. A. (2017). A review of the 0.1 reconnection rate problem. *Journal of Plasma Physics*, *83*(5), 715830501. https://doi.org/10.1017/S0022377817000666

Chang, C., Huang, K., Lu, Q., Sang, L., Lu, S., Wang, R., et al. (2021). Particle-in-cell simulations of electrostatic solitary waves in asymmetric magnetic reconnection. *Journal of Geophysical Research: Space Physics*, *126*(7), e2021JA029290. https://doi.org/10.1029/2021JA029290

Fu, X. R., Lu, Q. M., & Wang, S. (2006). The process of electron acceleration during collisionless magnetic reconnection. *Physics of Plasmas*, *13*(1), 012309. https://doi.org/10.1063/1.2164808

Gingell, I., Schwartz, S. J., Eastwood, J. P., Stawarz, J. E., Burch, J. L., Ergun, R. E., et al. (2020). Statistics of reconnecting current sheets in the transition region of earth's bow shock. *Journal of Geophysical Research: Space Physics*, *125*(1), e2019JA027119. https://doi.org/10.1029/2019JA027119

Guan, Y. (2024). Electron-only (Version V1). *Science Data Bank* [Dataset]. https://doi.org/10.57760/sciencedb.08229

Guan, Y., Lu, Q., Lu, S., Huang, K., & Wang, R. (2023). Reconnection rate and transition from ion-coupled to electron-only reconnection. *The Astrophysical Journal*, *958*(2), 172. https://doi.org/10.3847/1538-4357/ad05b8

Hesse, M., & Cassak, P. A. (2020). Magnetic reconnection in the space sciences: Past, present, and future. *Journal of Geophysical Research: Space Physics*, *125*(2), e2018JA025935. https://doi.org/10.1029/2018JA025935

Hesse, M., Neukirch, T., Schindler, K., Kuznetsova, M., & Zenitani, S. (2011). The diffusion region in collisionless magnetic reconnection. *Space Science Reviews*, *160*(1–4), 3–23. https://doi.org/10.1007/s11214-010-9740-1

Hesse, M., Zenitani, S., Kuznetsova, M., & Klimas, A. (2009). A simple, analytical model of collisionless magnetic reconnection in a pair plasma. *Physics of plasmas*, *16*(10), 102106. https://doi.org/10.1063/1.3246005

Huang, C., Lu, Q., Guo, F., Wu, M., Du, A., & Wang, S. (2015). Magnetic islands formed due to the Kelvin-Helmholtz instability in the outflow region of collisionless magnetic reconnection. *Geophysical Research Letters*, *42*(18), 7282–7286. https://doi.org/10.1002/2015GL065690

Huang, C., Lu, Q. M., & Wang, S. (2010). The mechanisms of electron acceleration in antiparallel and guide field magnetic reconnection. *Physics of Plasmas*, *17*(7), 072306. https://doi.org/10.1063/1.3457930

Hubbert, M., Qi, Y., Russell, C. T., Burch, J. L., Giles, B. L., & Moore, T. E. (2021). Electron-Only tail current sheets and their temporal evolution. *Geophysical Research Letters*, *48*(5), e2020GL091364. https://doi.org/10.1029/2020GL091364

Hubbert, M., Russell, C. T., Qi, Y., Lu, S., Burch, J. L., Giles, B. L., & Moore, T. E. (2022). Electron-only reconnection as a transition phase from quiet current sheet to traditional magnetotail reconnection. *Journal of Geophysical Research: Space Physics*, *127*(3), e2021JA029584. https://doi.org/10.1029/2021JA029584

Karimabadi, H., Daughton, W., & Scudder, J. (2007). Multi-scale structure of the electron diffusion region. *Geophysical Research Letters*, *34*(13), L13104. https://doi.org/10.1029/2007GL030306

Lin, J., & Forbes, T. G. (2000). Effects of reconnection on the coronal mass ejection process. *Journal of Geophysical Research*, *105*(A2), 2375–2392. https://doi.org/10.1029/1999JA900477

Liu, Y. H., Hesse, M., Guo, F., Daughton, W., Li, H., Cassak, P. A., & Shay, M. A. (2017). Why does steady-state magnetic reconnection have a maximum local rate of order 0.1? *Physical Review Letters*, *118*(8), 085101. https://doi.org/10.1103/PhysRevLett.118.085101

Lu, Q., Fu, H., Wang, R., & Lu, S. (2022). Collisionless magnetic reconnection in the magnetosphere. *Chinese Physics B*, *31*(8), 089401. https://doi.org/10.1088/1674-1056/ac76ab

Lu, Q., Huang, C., Xie, J., Wang, R., Wu, M., Vaivads, A., & Wang, S. (2010). Features of separatrix regions in magnetic reconnection: Comparison of 2-D particle-in-cell simulations and Cluster observations. *Journal of Geophysical Research*, *115*(A11), A11208. https://doi.org/10.1029/2010JA015713

Lu, S., Angelopoulos, V., Artemyev, A. V., Jia, Y., Chen, Q., Liu, J., & Runov, A. (2020a). Magnetic reconnection in a charged, electron-dominant current sheet. *Physics of Plasmas*, *27*(10), 102902. https://doi.org/10.1063/5.0020857

Lu, S., Lu, Q. M., Wang, R. S., Pritchett, P. L., Hubbert, M., Qi, Y., et al. (2022). Electron-only reconnection as a transition from quiet current sheet to standard reconnection in earth's magnetotail: Particle-in-cell simulation and application to MMS data. *Geophysical Research Letters*, *49*(11), e2022GL098547. https://doi.org/10.1029/2022GL098547

Lu, S., Wang, R. S., Lu, Q. M., Angelopoulos, V., Nakamura, R., Artemyev, A. V., et al. (2020b). Magnetotail reconnection onset caused by electron kinetics with a strong external driver. *Nature Communications*, *11*(1), 5049. https://doi.org/10.1038/s41467-020-18787-w

Man, H. Y., Zhou, M., Yi, Y. Y., Zhong, Z. H., Tian, A. M., Deng, X. H., et al. (2020). Observations of electron-only magnetic reconnection associated with macroscopic magnetic flux ropes. *Geophysical Research Letters*, *47*(19), e2020GL089659. https://doi.org/10.1029/2020GL089659

Masuda, S., Kosugi, T., Hara, H., Tsuneta, S., & Ogawara, Y. (1994). A loop-top hard X-ray source in a compact solar flare as evidence for magnetic reconnection. *Nature*, *371*(6497), 495–497. https://doi.org/10.1038/371495a0

Nagai, T., Shinohara, I., Fujimoto, M., Hoshino, M., Saito, Y., Machida, S., & Mukai, T. (2001). Geotail observations of the Hall current system: Evidence of magnetic reconnection in the magnetotail. *Journal of Geophysical Research*, *106*(A11), 25929–25949. https://doi.org/10.1029/2001ja900038

Ng, J., Chen, L., Bessho, N., Shuster, J., Burkholder, B., & Yoo, J. (2022). Electron-scale reconnection in three-dimensional shock turbulence. *Geophysical Research Letters*, *49*(15), e2022GL099544. https://doi.org/10.1029/2022GL099544

Phan, T. D., Eastwood, J. P., Shay, M. A., Drake, J. F., Sonnerup, B. U. O., Fujimoto, M., et al. (2018). Electron magnetic reconnection without ion coupling in Earth's turbulent magnetosheath. *Nature*, *557*(7704), 202–206. https://doi.org/10.1038/s41586-018-0091-5

Pritchett, P. L. (2001). Geospace Environment Modeling magnetic reconnection challenge: Simulations with a full particle electromagnetic code. *Journal of Geophysical Research*, *106*(A3), 3783–3798. https://doi.org/10.1029/1999ja001006

Pyakurel, P. S., Shay, M. A., Phan, T. D., Matthaeus, W. H., Drake, J. F., TenBarge, J. M., et al. (2019). Transition from ion-coupled to electron-only reconnection: Basic physics and implications for plasma turbulence. *Physics of Plasmas*, *26*(8), 082307. https://doi.org/10.1063/1.5090403

Sang, L., Lu, Q. M., Xie, J. L., Fan, F., Zhang, Q. F., Ding, W. X., et al. (2022). Energy dissipation during magnetic reconnection in the Keda linear magnetized plasma device. *Physics of Plasmas*, *29*(10), 102108. https://doi.org/10.1063/5.0090790

Shay, M. A., Drake, J. F., Rogers, B. N., & Denton, R. E. (2001). Alfvénic collisionless magnetic reconnection and the Hall term. *Journal of Geophysical Research*, *106*(A3), 3759–3772. https://doi.org/10.1029/1999ja001007

Shay, M. A., Drake, J. F., & Swisdak, M. (2007). Two-scale structure of the electron dissipation region during collisionless magnetic reconnection. *Physical Review Letters*, *99*(15), 155002. https://doi.org/10.1103/PhysRevLett.99.155002

Shi, P. Y., Srivastav, P., Barbhuiya, M. H., Cassak, P. A., Scime, E. E., & Swisdak, M. (2022a). Laboratory observations of electron heating and non-maxwellian distributions at the kinetic scale during electron-only magnetic reconnection. *Physical Review Letters*, *128*(2), 025002. https://doi.org/10.1103/PhysRevLett.128.025002

Shi, P. Y., Srivastav, P., Barbhuiya, M. H., Cassak, P. A., Scime, E. E., Swisdak, M., et al. (2022b). Electron-only reconnection and associated electron heating and acceleration in PHASMA. *Physics of Plasmas*, *29*(3), 032101. https://doi.org/10.1063/5.0082633

Stawarz, J. E., Eastwood, J. P., Phan, T. D., Gingell, I. L., Pyakurel, P. S., Shay, M. A., et al. (2022). Turbulence-driven magnetic reconnection and the magnetic correlation length: Observations from Magnetospheric Multiscale in Earth's magnetosheath. *Physics of Plasmas*, *29*(1), 012302. https://doi.org/10.1063/5.0071106

Stawarz, J. E., Eastwood, J. P., Phan, T. D., Gingell, I. L., Shay, M. A., Burch, J. L., et al. (2019). Properties of the turbulence associated with electron-only magnetic reconnection in earth's magnetosheath. *The Astrophysical Journal Letters*, *877*(2), L37. https://doi.org/10.3847/2041-8213/ab21c8

Torbert, R. B., Burch, J. L., Phan, T. D., Hesse, M., Argall, M. R., Shuster, J., et al. (2018). Electron-scale dynamics of the diffusion region during symmetric magnetic reconnection in space. *Science*, *362*(6421), 1391–1395. https://doi.org/10.1126/science.aat2998

Wang, R., Lu, Q., Nakamura, R., Baumjohann, W., Huang, C., Russell, C. T., et al. (2018). An electron-scale current sheet without bursty reconnection signatures observed in the near-Earth tail. *Geophysical Research Letters*, *45*(10), 4542–4549. https://doi.org/10.1002/2017GL076330

Wang, R. S., Lu, Q. M., Lu, S., Russell, C. T., Burch, J. L., Gershman, D. J., et al. (2020). Physical implication of two types of reconnection electron diffusion regions with and without ion-coupling in the magnetotail current sheet. *Geophysical Research Letters*, *47*(21), e2020GL088761. https://doi.org/10.1029/2020GL088761

Wang, S., & Lu, Q. M. (2019). *Collisionless magnetic reconnection*. Science Press.

Yamada, M., Kulsrud, R., & Ji, H. T. (2010). Magnetic reconnection. *Reviews of Modern Physics*, *82*(1), 603–664. https://doi.org/10.1103/RevModPhys.82.603